

## High-pressure melting of lead

F. Cricchio,<sup>1</sup> A. B. Belonoshko,<sup>2,3</sup> L. Burakovsky,<sup>4</sup> D. L. Preston,<sup>5</sup> and R. Ahuja<sup>1,2</sup>

<sup>1</sup>Condensed Matter Theory Group, Department of Physics, P.O. Box 530, Uppsala University, SE-75121 Uppsala, Sweden

<sup>2</sup>Applied Materials Physics, Department of Material Science and Engineering, The Royal Institute of Technology (KTH), SE-10044 Stockholm, Sweden

<sup>3</sup>Condensed Matter Theory Group, AlbaNova University Center, The Royal Institute of Technology, SE-106 91 Stockholm, Sweden

<sup>4</sup>Theoretical Division, Los Alamos National Laboratory, Los Alamos, New Mexico 87545, USA

<sup>5</sup>Physics Division, Los Alamos National Laboratory, Los Alamos, New Mexico 87545, USA

(Received 13 September 2005; published 26 April 2006)

The melting curve of the hexagonal close-packed (hcp) phase of lead (Pb) has been determined over a wide pressure range using both *ab initio* molecular dynamics (AIMD) simulations and classical molecular dynamics (CMD) employing an effective pair potential. The AIMD simulations are based on a density functional theory (DFT) in the generalized gradient approximation (GGA). The Pb melting curve, constructed using a well-established theoretical scheme, is in excellent agreement with the AIMD results. Our calculated equation of state (EOS) of hcp Pb is in excellent agreement with experimental data up to 40 GPa. Our melting curve agrees very well with melting temperatures obtained in both shock-wave and diamond-anvil cell (DAC) experiments, but at higher pressures our curve lies between the two data sets.

DOI: [10.1103/PhysRevB.73.140103](https://doi.org/10.1103/PhysRevB.73.140103)

PACS number(s): 64.10.+h, 64.70.Dv, 71.15.Pd

The high-pressure melting of several elements, in particular Mo and Fe, remains controversial despite extensive experimental and theoretical studies. In the case of Mo, the melting curve obtained from *ab initio* molecular dynamics (AIMD) simulations<sup>1</sup> is substantially higher than that determined in diamond-anvil cell (DAC) experiments to 100 GPa.<sup>2</sup> Similarly for Fe, the DAC melting curve<sup>3</sup> lies significantly below the melting curve obtained from the shock-wave experiments.<sup>4,5</sup> A recent AIMD calculation<sup>6</sup> showed good agreement with the shock-wave data.<sup>4</sup>

In this paper, we determine the melting curve of Pb to 100 GPa. Lead is of considerable interest because, like Mo and Fe, shock-wave and DAC measurements of its high-pressure melting temperatures ( $T_m$ ) are inconsistent. In 1990, Godwal *et al.*<sup>7</sup> measured the Pb melting curve to a pressure ( $P$ ) of 100 GPa, where  $T_m \sim 4000$  K, by means of a laser-heated DAC. More recently, Pb melting temperatures were measured by Partouche-Sebban *et al.*<sup>8</sup> utilizing pyrometry and reflectometry diagnostics in shock-wave experiments. Their values of  $T_m$  are in very good agreement with the theoretical results of Pelissier<sup>9</sup> based on a model potential. However, the  $T_m$  data obtained by Partouche-Sebban *et al.* are substantially higher than the DAC data of Godwal *et al.*<sup>7</sup> Our aim is to accurately calculate the melting curve of Pb by means of AIMD, and to discriminate between the widely differing shock-wave and DAC data.

We pause to mention some facts about Pb pertinent to this study. Lead is highly compressible,<sup>10</sup> and should, therefore, exhibit phenomena that for other substances are typically seen at higher  $P$ . Its melting temperature at ambient  $P$  is 600.6 K.<sup>10,11</sup> The  $T=300$  K isotherm of lead has been extensively studied both experimentally and theoretically.<sup>12–16</sup> Lead undergoes only one solid-solid transition, fcc  $\rightarrow$  hcp, at pressures below 100 GPa (Refs. 17 and 18); the transition occurs at 13 GPa at room temperature.<sup>17</sup> Diffraction studies on compressed Pb show that it undergoes a second phase transition from hcp to bcc at  $P=109$  GPa.<sup>18</sup>

We determine the melting curve of Pb up to 100 GPa by means of three approaches: (1) AIMD simulations; (2) classical molecular dynamics (CMD) simulations using an effective pair potential  $\phi(r)$  obtained from AIMD data; (3) a well-established theoretical scheme developed by Burakovsky and Preston.<sup>19</sup>

Before simulating Pb melting, we first investigated the reliability of the AIMD method by calculating the  $T=0$  isotherm of the hcp phase as well as the fcc  $\rightarrow$  hcp and hcp  $\rightarrow$  bcc transition pressures at  $T=0$ . The calculations were done with the Vienna *ab initio* Simulation Package (VASP).<sup>20</sup> Pb in the fcc, hcp, and bcc structures was studied within the framework of a full-potential frozen-core all-electron projected augmented wave method,<sup>21</sup> as implemented in VASP,<sup>20</sup> with ionic relaxations taken into account for the hcp phase. In these calculations and in the subsequent AIMD simulations, the energy cutoff  $E_c$  for the plane wave basis set was chosen equal to 98.0 eV. Exchange and correlation effects were treated through the generalized gradient approximation of Perdew *et al.*<sup>22</sup> The integration over the Brillouin zone was done on special  $k$  points determined by the Monkhorst-Pack method.<sup>23</sup> All necessary convergence tests were performed. For the  $T=0$  calculations, the required energy convergence was achieved using 104 irreducible  $k$  points for the fcc and bcc structures, and 133 irreducible  $k$  points for the hcp case. For the AIMD, we employed a single  $k$  point centered at the  $\Gamma$  point. The calculated  $T=0$  isotherm (Fig. 1) is in very good agreement with the experiment<sup>12–14</sup> and the earlier first-principles calculations.<sup>15,16</sup> As follows from the calculated enthalpies for a number of phases, Pb is stable in the fcc structure at  $T=0$  up to 14 GPa where it transforms to the hcp phase. This result is in excellent agreement with the measurements<sup>17</sup> and the theoretical results.<sup>15</sup> We have also calculated the  $T=0$  hcp  $\rightarrow$  bcc transition pressure to be 121 GPa, which compares favorably with the results of previous investigations.<sup>15,18</sup> Given this agreement, our AIMD

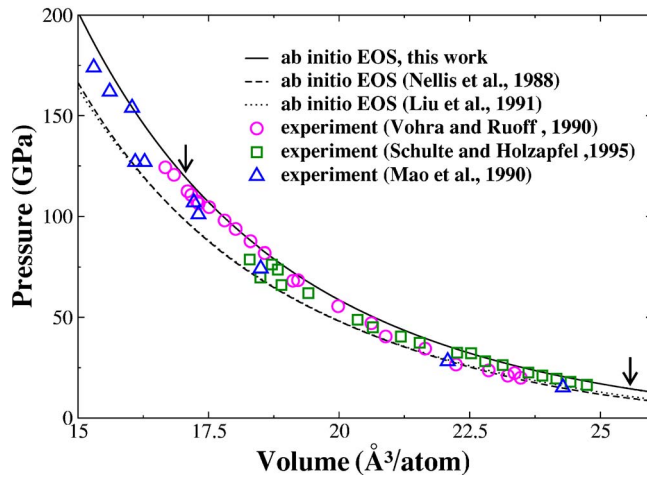


FIG. 1. (Color online) Comparison of the experimental<sup>12-14</sup> and calculated<sup>15,16</sup>  $T=0$  isotherms for the hcp phase of Pb. The arrows show the calculated transition pressures from the fcc to hcp, and from the hcp to bcc phases of Pb.

simulations of Pb melting are expected to be highly reliable.

We have conducted our AIMD simulations of the melting of Pb in a  $NVE$  ensemble ( $N$  number of particles,  $V$  volume,  $E$  energy) at four  $V$ : 31.63, 22.81, 19.91, and 18.70  $\text{\AA}^3/\text{atom}$ . For the largest volume, we used  $N=108$  atoms arranged in an ideal fcc lattice ( $3 \times 3 \times 3$  conventional unit fcc cells), but for the other three volumes we chose  $N=96$  atoms arranged in an ideal hcp structure ( $4 \times 4 \times 3$  primitive hcp cells). These volumes correspond roughly to pressures of 0, 30, 60, and 80 GPa, respectively, at  $T=0$ . At these volumes, we performed AIMD simulations at a number of temperatures. We used a time step,  $\tau$ , of 2 fs for all four volumes. Two thousand  $\tau$  were used for equilibration, during which velocities were scaled to the desired temperature every  $2\tau$ . Subsequently, the system evolved independently for other 2000 time steps. With increasing  $T$ , we observed a discontinuous change in  $P$  and structure; see the calculated radial distribution functions (RDF) in Fig. 2. Close examination of the structural changes, as well as a dramatic increase in atomic mobility, confirmed that this discontinuous behavior was due to melting. The four instability points ( $P, T_i^{\text{AIMD}}$ ) obtained by AIMD are (2,850), (39,2910), (74,4340), and (95,4760), where pressures are in GPa and temperatures are in degrees K; these points are shown as filled circles in Fig. 3. The discontinuous pressure changes observed in our computer experiments occur at instability temperatures  $T_i$  that exceed the melting temperatures  $T_m$ , a phenomenon known as overheating. The degree of overheating,  $\delta=(T_i-T_m)/T_i$ , usually varies from about 10% at low  $P$  to at most 23% at high  $P$ . This empirical observation is based on molecular dynamics simulations for a number of materials.<sup>24-28</sup>

Ideally, we would calculate the Pb melting curve by AIMD using the two-phase method.<sup>24</sup> In the two-phase method, presimulated solid and liquid regions are brought together, forming an interface in order to remove the barrier in the Gibbs free energy that prevents melting and crystallization. However, the two-phase scheme requires a considerably larger  $N$ , which would have made our AIMD simulations too time consuming.

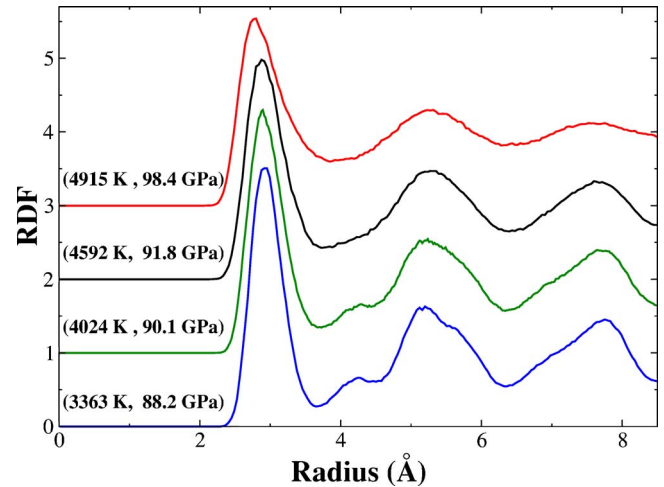


FIG. 2. (Color online) RDFs of Pb calculated for  $V=18.70 \text{\AA}^3/\text{atom}$  by AIMD in  $NVE$  at a number of  $T_s$ . The RDFs are shifted up by 1, 2, and 3. The RDF at 4915 K is typical of liquids, while other RDFs are typical of solids.

The AIMD simulation at  $V=31.63 \text{\AA}^3/\text{atom}$  gave  $T_i=850$  K at a pressure of 2.0 GPa. Using  $(dT_m/dP)_0=77.8 \pm 5.5 \text{ K/GPa}$  (Ref. 10) and  $T_m(0)=600.6$  K we obtain  $T_m(2.0 \text{ GPa})=756 \pm 11$  K. Hence, at 2.0 GPa we have  $\delta=0.11$ .

We evaluated  $\delta$  at the smallest volume,  $V=18.70 \text{\AA}^3/\text{atom}$ , by performing one- and two-phase CMD simulations to obtain  $T_i$  and  $T_m$ , respectively. All CMD simulations were carried out using the MOLDY package<sup>29</sup> with an effective spherical pair potential  $\phi(r)$  obtained from particle positions and potential energy values saved during AIMD runs. At high  $T$ , the atomic vibrations render the interaction effectively angle independent, thus justifying the assumed spherical symmetry of  $\phi$ . We determined the potential  $\phi(r_j)$  at distance  $r_j$  by minimizing the system of equations  $\sum_j^N b \|n_{ij}\phi(r_j) - E_i\|^2$ , where  $n_{ij}$  is the number of particles lying between  $r_j$  and  $r_j + \delta r$  in the system configuration  $i$ , where  $E_i$

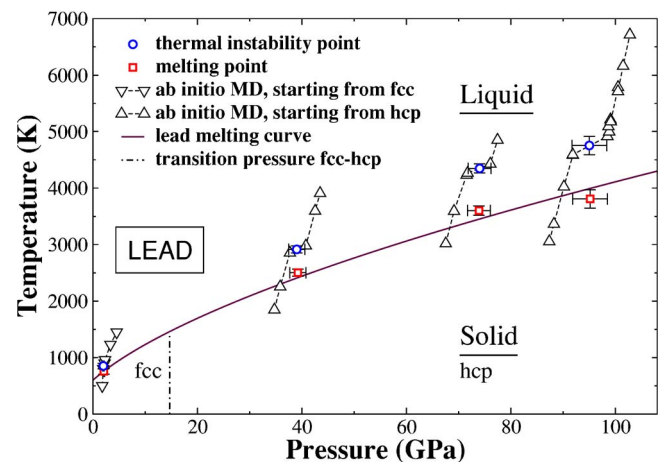


FIG. 3. (Color online) Calculated phase diagram of Pb. The triangles are Pb isochores calculated by AIMD. The melting points were determined using the two-phase method (Ref. 24) and fitted by the Simon functional form.

is the corresponding potential energy, and  $N_b$  is the number of distance intervals. We used 1000 configurations saved during the AIMD equilibration stage. We fitted the points  $\phi(r_j)$  to the function  $\phi(r)=Ae^{-Br}$ . Assuming that only the repulsive term in the interaction is important at high  $P$ , we obtained the values  $A=3.48$  keV and  $B=2.9755 \text{ \AA}^{-1}$ . We calculated  $T_m^{CL}$  at pressures of 90 and 100 GPa by carrying out two-phase CMD simulations in the  $NPT$  ensemble by means of a Raman-Parrinello barostat and a Nosé-Hoover thermostat.<sup>29</sup> Our system was comprised of 1176 Pb atoms, half in the liquid state and half in the hcp phase. We performed 50 000 time steps  $\tau$ , where 10 000 $\tau$  were allotted to equilibration, with  $\tau=2.0$  fs. We calculated a thermal instability point  $(P, T_i^{CL})$  by CMD in a  $NVE$  ensemble following the same one-phase procedure used in the AIMD runs. Setting  $N=96$ ,  $V=18.70 \text{ \AA}^3/\text{atom}$ , and  $\tau=2.0$  fs, we performed the same number of  $\tau$  as in the AIMD simulations. Melting occurred in the same  $P$ - $T$  range as in the AIMD case, which shows that the effective  $\phi(r)$  we used is reliable. We found  $\delta=(T_i^{CL}-T_m^{CL})/T_i^{CL}=0.20$  at  $P=93.52$  GPa, the pressure at which  $T_i^{CL}$  was calculated, using linear interpolation between 90 and 100 GPa to obtain  $T_m^{CL}$  at 93.52 GPa.

The degree of overheating at 74 GPa ( $V=19.91 \text{ \AA}^3/\text{atom}$ ) was calculated using the interatomic potential obtained from AIMD at 95 GPa, since these pressures differ by only  $\sim 25\%$ . One-phase CMD calculations were done for systems comprised of 96, 392, and 1176 atoms. The degree of overheating was 0.17 in each of the three cases, and so we estimate  $\delta=0.17$  at 74 GPa. Finally, to estimate  $\delta$  at 39 GPa ( $V=22.81 \text{ \AA}^3/\text{atom}$ ), which is too low in pressure to apply the repulsive potential  $\phi(r)=A \exp(-Br)$ , we average the degree of overheating at 2 and 74 GPa to obtain 14%.

We reduced the AIMD instability temperatures 850, 2910, 4340, and 4760 K by 11%, 14%, 17%, and 20%, respectively, and then fit the Simon functional form to the resulting temperatures to obtain  $T_m(P)=600.6(1+P/4.46)^{0.61}$ . This gives  $dT_m(P)/dP=82.1$  K/GPa at  $P=0$ , in agreement with the experimental result  $77.8 \pm 5.5$ .<sup>10</sup>

We then constructed the melting curve of Pb using the well-established theoretical scheme developed by Burakovsky and Preston,<sup>19</sup> in which a theoretical melting curve of any substance can be derived as function of density,  $\rho$ . This scheme has been tested on a number of substances, both simple monatomic<sup>1,19</sup> and complex polyatomic, such as magnesium silicate,<sup>30</sup> and very good agreement with the experiment has been found in all cases. The scheme reduces to the calculation of three unknown parameters,  $\gamma_1$ ,  $\gamma_2$ , and  $q$ , for the effective representation of the Grüneisen parameter,  $\gamma(\rho)=1/2 + \gamma_1/\rho^{1/3} + \gamma_2/\rho^q$ , and the subsequent integration of the Lindemann equation,  $d \ln T_m(\rho)/d \ln \rho=2[\gamma(\rho)-1/3]$ , to obtain the melting curve in the form

$$T_m(\rho) = T_m(\rho_m) \left( \frac{\rho}{\rho_m} \right)^{1/3} \exp \left[ 6\gamma_1 \left( \frac{1}{\rho_m^{1/3}} - \frac{1}{\rho^{1/3}} \right) + \frac{2\gamma_2}{q} \left( \frac{1}{\rho_m^q} - \frac{1}{\rho^q} \right) \right], \quad (1)$$

where  $T_m(\rho_m)$  is the melting temperature at a given reference

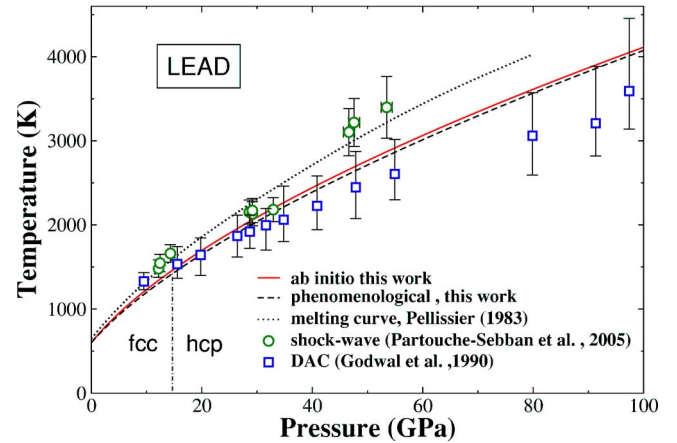


FIG. 4. (Color online) Experimental data and theory on the phase state of Pb as a function of  $P$  and  $T$ . Accurate calculations with increased energy cutoff for the plane wave basis set and increased number of  $k$  points showed that the maximum error on melting temperatures is 200 K at the highest  $P$  (Ref. 32).

density  $\rho_m$ , which is conveniently chosen to be that at the  $P=0$  melting point. The values of  $\gamma_1$ ,  $\gamma_2$ , and  $q$  are obtained by solving a system of three equations:<sup>19</sup> (i)  $\gamma(\rho_a)=\gamma_a$ , (ii)  $\gamma(\rho_b)=\gamma_b$ , where  $a$  and  $b$  are two reference states, and (iii) the one-component plasma limiting form of Eq. (1).<sup>19</sup> Using (in  $\text{g cm}^{-3}$ )  $\rho_a=\rho(T=0, P=0)=11.58$ ,  $\rho_b=\rho_m \equiv \rho(T=T_m=600.6 \text{ K}, P=0)=11.01$ ,<sup>11</sup>  $\gamma_a=2.7$ ,<sup>31</sup> and  $\gamma_b=3.0$ ,<sup>10</sup> we obtain  $\gamma_1=3.03$ ,  $\gamma_2=6.11 \cdot 10^5$ ,  $q=5.5$ . To calculate the theoretical melting curve of Pb in  $T$ - $P$  coordinates, we now use equation of states (EOSs) for the fcc, hcp, and bcc phases of Pb (Ref. 12) to convert Eq. (1) into the corresponding  $T_m=T_m(P)$  form. This is done by choosing 35 equally spaced  $\rho$  points from 11.0 to 28.0  $\text{g cm}^{-3}$  (the corresponding pressures range from  $P \approx 0$  to  $P \approx 5$  Mbar) and calculating the corresponding  $P$  based on  $T_m$  from Eq. (1) and the EOS. Now, fitting the Simon functional form to the set of 35 data points, with the constraint that  $T_m(P=0)=600.6$  K, leads to ( $P$  in GPa)  $T_m(P)=600.6(1+P/5.03)^{0.63}$ , for  $0 \leq P \leq 500$ . This gives  $dT_m(P)/dP=75.2$  K/GPa at  $P=0$ , in agreement with Ref. 10.

The melting curves of lead obtained with AIMD simulations and calculated in the phenomenological approach are shown in Fig. 4, along with the experimental data<sup>7,8</sup> and the earlier theoretical results of Pellissier.<sup>9</sup> Agreement between the AIMD and the phenomenological melting curves is excellent. The melting curve of Godwal *et al.*<sup>7</sup> is in very good agreement with our results up to 40 GPa, but it is lower than ours for higher  $P$ . However, since its uncertainties are quite large (20%–30% in the range 80–100 GPa), our results are within the error bars of Ref. 7 in the range 50–100 GPa. The melting curve of Partouche-Sebban *et al.*<sup>8</sup> is in very good agreement with our results up to 40 GPa, and yet in reasonable agreement up to 60 GPa. Our melting curve is also in reasonable agreement with the earlier calculations of Pellissier,<sup>9</sup> who used a model potential.

To conclude, we have obtained the melting temperatures of the hcp phase of lead up to 100 GPa by applying both density functional theory-based AIMD in the Born-Oppen-

heimer approximation and CMD techniques with an effective pair potential. We have also performed the calculation of the Pb melting curve in a phenomenological approach, and it turned out to be in excellent agreement with that obtained from AIMD. Our results are in good agreement, up to 40 GPa, with both the shock-wave data<sup>8</sup> and the DAC measurements.<sup>7</sup> However, for  $P$  in the range 40–100 GPa, our melting temperatures are higher than those from the DAC, yet within their error bars, and lower than those from the shock-wave measurements. A similar situation occurs in the case of iron where inconsistencies between the “low”

melting curve measured in the DAC,<sup>3</sup> and the “high” one obtained from shock-wave experiments<sup>4,5</sup> are notorious. A recent calculation by means of quasi-AIMD (Ref. 6) showed good agreement with shock-wave data<sup>4</sup> at lower pressures. At the highest pressures, however, the quasi-AIMD curve is below the shock-wave data<sup>4</sup> and above the DAC points,<sup>3</sup> as in the case of Pb. Also, for Mo (Ref. 1) the AIMD melting curve is significantly higher than the DAC melting curve.<sup>2</sup> However, we point out that comparisons between the DAC and shock-wave data should be made with caution, since the two techniques are significantly different.

- <sup>1</sup>A. B. Belonoshko, S. I. Simak, A. E. Kochetov, B. Johansson, L. Burakovsky, and D. L. Preston, *Phys. Rev. Lett.* **92**, 195701 (2004).
- <sup>2</sup>D. Errandonea, B. Schwager, R. Ditz, C. Gessmann, R. Boehler, and M. Ross, *Phys. Rev. B* **63**, 132104 (2001).
- <sup>3</sup>R. Boehler, *Nature (London)* **363**, 534 (1993).
- <sup>4</sup>C. S. Yoo, N. C. Holmes, M. Ross, D. J. Webb, and C. Pike, *Phys. Rev. Lett.* **70**, 3931 (1993).
- <sup>5</sup>J. M. Brown and R. G. McQueen, *J. Geophys. Res.* **95**, 21713 (1986).
- <sup>6</sup>A. B. Belonoshko, R. Ahuja, and B. Johansson, *Phys. Rev. Lett.* **84**, 3638 (2000); A. B. Belonoshko, B. Johansson, and R. Ahuja, *Nature (London)* **424**, 1032 (2003).
- <sup>7</sup>B. K. Godwal, C. Meade, R. Jeanloz, A. Garcia, A. Y. Liu, and M. L. Cohen, *Science* **248**, 462 (1990).
- <sup>8</sup>D. Partouche-Sebban, J. L. Pelissier, F. G. Abeyta, W. W. Anderson, M. E. Byers, D. Dennis-Koller, J. S. Esparza, R. S. Hixson, D. B. Holtkamp, B. J. Jensen, J. C. King, P. A. Rigg, P. Rodriguez, D. L. Shampine, J. B. Stone, D. T. Westley, S. D. Borrer, and C. A. Kruschwitz, *J. Appl. Phys.* **97**, 43521 (2005).
- <sup>9</sup>J. L. Pelissier, *Physica A* **126**, 271 (1984).
- <sup>10</sup>P. W. Mirwald and G. C. Kennedy, *J. Phys. Chem. Solids* **37**, 795 (1976).
- <sup>11</sup>D. C. Wallace, *Statistical Physics of Crystals and Liquids* (World Scientific, Singapore, 2002).
- <sup>12</sup>Y. K. Vohra and A. L. Ruoff, *Phys. Rev. B* **42**, 8651 (1990).
- <sup>13</sup>O. Schulte and W. B. Holzapfel, *Phys. Rev. B* **52**, 12636 (1995).
- <sup>14</sup>H. K. Mao, Y. Wu, J. F. Shu, J. Z. Hu, R. J. Hemley, and D. E. Cox, *Solid State Commun.* **74**, 1027 (1990).
- <sup>15</sup>A. Y. Liu, A. Garcia, M. L. Cohen, B. K. Godwal, and R. Jeanloz, *Phys. Rev. B* **43**, 1795 (1991).
- <sup>16</sup>W. J. Nellis, J. A. Moriarty, A. C. Mitchell, M. Ross, R. G. Dandrea, N. W. Ashcroft, N. C. Holmes, and G. R. Gathers, *Phys. Rev. Lett.* **60**, 1414 (1988).
- <sup>17</sup>T. Takahashi, H. K. Mao, and W. A. Bassett, *Science* **165**, 1352 (1969).
- <sup>18</sup>C. A. Vanderborgh, Y. K. Vohra, H. Xia, and A. L. Ruoff, *Phys. Rev. B* **41**, 7338 (1990).
- <sup>19</sup>L. Burakovsky and D. L. Preston, *J. Phys. Chem. Solids* **65**, 1581 (2004).
- <sup>20</sup>G. Kresse and J. Furthmüller, *Comput. Mater. Sci.* **6**, 15 (1996).
- <sup>21</sup>P. E. Blöchl, *Phys. Rev. B* **50**, 17953 (1994).
- <sup>22</sup>J. P. Perdew, J. A. Chevary, S. H. Vosko, K. A. Jackson, M. R. Pederson, D. J. Singh, and C. Fiolhais, *Phys. Rev. B* **46**, 6671 (1992).
- <sup>23</sup>H. J. Monkhorst and J. D. Pack, *Phys. Rev. B* **13**, 5188 (1972).
- <sup>24</sup>A. B. Belonoshko, *Geochim. Cosmochim. Acta* **58**, 4039 (1994); A. B. Belonoshko, *Phys. Chem. Miner.* **25**, 138 (1998).
- <sup>25</sup>A. B. Belonoshko, R. Ahuja, O. Eriksson, and B. Johansson, *Phys. Rev. B* **61**, 3838 (2000).
- <sup>26</sup>A. B. Belonoshko, R. Ahuja, and B. Johansson, *Phys. Rev. Lett.* **84**, 3638 (2000).
- <sup>27</sup>A. B. Belonoshko and L. S. Dubrovinsky, *Am. Mineral.* **81**, 303 (1996).
- <sup>28</sup>P. M. Agrawal, B. M. Rice, and D. L. Thompson, *J. Chem. Phys.* **118**, 9680 (2003).
- <sup>29</sup>K. Refson, *MOLDY*, Release 2.16, 2001. A general purpose molecular dynamics code, available for free at <http://www.earth.ox.ac.uk/keithr/moldy.html>.
- <sup>30</sup>A. B. Belonoshko, N. V. Skorodumova, A. Rosengren, R. Ahuja, B. Johansson, L. Burakovsky, and D. L. Preston, *Phys. Rev. Lett.* **94**, 195701 (2005).
- <sup>31</sup>G. K. White, *Philos. Mag.* **7**, 271 (1962).
- <sup>32</sup>D. Alfé, M. J. Gillan, and G. D. Price, *J. Chem. Phys.* **116**, 6170 (2002).